Design Equations for Flexural Capacity of Concrete Beams Reinforced with Glass Fiber–Reinforced Polymer Bars

Weichen Xue[1]; Fei Peng[2]; and Qiaowen Zheng[3]

Abstract: The flexural failure mode of concrete beams reinforced with glass fiber-reinforced polymer (GFRP) bars changes from GFRP rupture to concrete crushing as the reinforcement ratio increases. Due to the uncertainties of material strengths, assumptions made in analysis, and variations in locations of reinforcements and dimensions of sections, there is a transition region where both flexural failure modes are possible. An iterative procedure is required when GFRP rupture governs the design. To avoid this iteration, the current American standard adopts a simplified but conservative procedure. In this study, the upper bound of the reinforcement ratio for beams in the transition region is revised. Moreover, a simplified yet rational design equation for calculating the flexural capacity of under-reinforced beams is proposed based on rigorous sectional analyses. Also, alternative design equations based on regression analyses are developed to predict the flexural capacity of beams in the transition region and over-reinforced beams, respectively. Moreover, the performance of the proposed equations is compared to that of design equations of recent standards by comparing their predictions with experimental results of 173 GFRP reinforced concrete beams collected from the available literature. **DOI: 10.1061/(ASCE)CC.1943-5614.0000630.**

Author keywords: Glass fiber-reinforced polymer (GFRP) bar; Concrete beam; Failure mode; Flexural capacity; Transition region; Design equation.

Introduction

The corrosion of steel reinforcement in concrete structures is one of the major challenges facing the construction industry. When exposed to aggressive environments, such as deicing salts and marine environments, concrete infrastructure is especially susceptible to corrosion. Decades of research have shown that substitution of steel bars with fiber-reinforced polymer (FRP) reinforcements is an alternative solution (Nanni et al. 2014). In addition to a high resistance to corrosion, FRP reinforcements have characteristics that include a high strength-weight ratio, outstanding fatigue resistance, lower elastic modulus compared to steel, and a linear stress-strain relationship. At present, commercially available fibers include glass, carbon, aramid, and basalt, and bars using them are termed GFRP, CFRP, AFRP, and BFRP bars, respectively. In practice, GFRP bars are widely used as reinforcement for concrete members in lieu of conventional steel reinforcing bars due to their relative low cost.

Over the last two decades, a considerable number of experimental studies (Nanni 1993; Benmokrane et al. 1996; Yost et al. 2001; Kassem et al. 2011; El-Nemr et al. 2013) have been carried out to investigate the flexural responses of GFRP reinforced concrete (RC) beams. These experimental studies have shown that GFRP RC members fail in flexure in a brittle manner, either due to concrete crushing (compression failure mode) or rupture of the GFRP bars (tension failure mode). At limited state, the compression failure mode is the recommended failure mechanism since it is more progressive and has a higher degree of deformability [Nanni 1993; ACI Committee 440 (ACI 2006)]. Nevertheless, design practice indicates that for some members, such as bridge deck GFRP RC slabs, tension failure mode is a common practice (Choi et al. 2008).

As GFRP bars possess mechanical and bond properties different from steel bars, the analytical procedure developed for the design of concrete structures reinforced with steel bars is not necessarily applicable to those reinforced with GFRP bars (Nanni 1993; Xue et al. 2008). The desired failure mode in a traditional steel-reinforced beam is yielding of the tension steel, followed by eventual crushing of the concrete in the compression zone of the member. Because steel reinforcement is a typical elastic-plastic material and exhibits a long yield plateau, this desired failure mode can be always implemented in the steel-reinforced beam design practice. Since GFRP reinforcing bars are linear elastic to failure, a desired steel-like failure only occurs in the balanced point where rupture of GFRP and crushing of concrete occur simultaneously in GFRP RC beams. Theoretically, the distinction between compression failure mode and tension failure mode is achieved through the balanced reinforcement ratio ρ_{fb}. However, due to uncertainties of material strengths, assumptions in analysis, and variations in locations of reinforcements and dimensions of concrete sections (MacGregor 1997), the actual flexural failure mode may differ from the predicted one. That is, there is a transition region where compression failure mode and tension failure mode are possible. ACI 440.1R-06 (ACI 2006) suggested that the upper bound of reinforcement ratio of beams in the transition region ρ^* was taken as $1.4\rho_{fb}$. Similarly, other researchers (Vijay and GangaRao 2001; Yost and Gross 2002) proposed a reinforcement ratio of $1.33\rho_{fb}$. Lau and Pam (2010) compared ρ_{fb} at the design stage with that at the testing stage for GFRP RC beams and suggested that the upper bound of $1.4\rho_{fb}$ for the transition region should be increased. From the aforementioned discussions, it is concluded that there is no universally accepted value of ρ^* and that this value should be further investigated.

[1]Professor, Dept. of Structural Engineering, Tongji Univ., Siping Rd., 1239, Shanghai 200092, China (corresponding author). E-mail: xuewc@tongji.edu.cn

[2]Ph.D. Candidate, Dept. of Structural Engineering, Tongji Univ., Shanghai 200092, China. E-mail: pengfei2009@hnu.edu.cn

[3]Design Engineer, Dept. of Structural Engineering, Tongji Univ., Shanghai 200092, China. E-mail: qiaowenzheng@hotmail.com

Note. This manuscript was submitted on February 7, 2015; approved on August 6, 2015; published online on October 19, 2015. Discussion period open until March 19, 2016; separate discussions must be submitted for individual papers. This paper is part of the ***Journal of Composites for Construction***, © ASCE, ISSN 1090-0268.

Based on a review of existing FRP RC design guidelines [Fédération Internationale du Béton (FIB 2007); ACI Committee 440 (ACI 2006); Canadian Standards Association (CSA 2002); Italian National Research Council (CNR) 2006; ISIS Canada 2007] for determining the flexural strength of FRP RC beams, it is found that FIB task group 9.3 (FIB 2007) and ISIS Canada (2007) require an iterative procedure for under-reinforced ($\rho_f < \rho_{fb}$) beams, because an under-reinforced section will fail due to rupture of the FRP bars in tension before the concrete has reached its ultimate strain ε_{cu}. This iterative procedure based on the three principles of mechanics of deformable bodies (equilibrium conditions, compatibility conditions, and constitutive conditions) is regarded as accurate but too complex to be efficiently used in normal calculations in design offices (Bank 2006). To avoid this iteration, ACI 440.1R-06 (ACI 2006) adopts a simplified procedure based on the balanced failure condition in which the concrete reaches the ultimate compressive strain ε_{cu}. This simplification, however, assumes a constant maximum value for the depth of the compressive stress block (Choi et al. 2008), which means a minimum lever arm of the couple force. Accordingly, ACI 440.1R-06 (ACI 2006) is regarded as conservation when dealing with flexural failure due to FRP rupture (Bank 2006; Nanni et al. 2014). It should be mentioned that the assumed stress distribution in the concrete conflicts with the force equilibrium. In addition, regarding the flexural capacity of over-reinforced beams ($\rho_f \geq \rho^*$), experimental results generally showed higher loads than those predicted by ACI 440 (ACI 2006) design equations (Thériault and Benmokrane 1998; Wang and Belarbi 2005; Barris et al. 2009). This may be attributed to the fact that the ACI 440 (ACI 2006) equation ignores the reinforcement in the compression zone and the maximum concrete crushing strain, ε_{cu}, can reach higher values than the assumed value of 0.003 in analysis (Barris et al. 2009; Kara and Ashour 2012). Moreover, when estimating the flexural capacity of the beams in the transition region ($\rho_{fb} \leq \rho_f < \rho^*$), current design equations based on the assumption of concrete crushing may overestimate the load capacity of the beams in transition (Xue et al. 2009) Therefore, it is necessary to develop simplified and accurate calculating design equations for predicting the flexural capacity of under-reinforced beams, beams in the transition region, and over-reinforced beams, respectively.

In this paper, the upper bound of reinforcement ratio for GFRP RC beams in the transition region is revised. Then, rigorous sectional analyses based on the three principles of mechanics of deformable bodies are carried out to obtain a simplified and rational design equation for calculating the flexural capacity of the under-reinforced beams. Subsequently, simple yet improved design equations based on regression analyses are developed to calculate the flexural capacity of GFRP RC beams in the transition and over-reinforced beams, respectively. Finally, the accuracy of the proposed equations, ACI 440 (ACI 2006) equations and FIB Task Group 9.3 (FIB 2007) equations is evaluated by comparing their predictions with experimental results of 173 GFRP RC beams available in the literature.

Design Equations for Nominal Flexural Strength

Basic Assumption

Referring to ACI 440.1R-06 (ACI 2006), the following assumptions are made in calculating the nominal flexural strength of RC beams reinforced with GFRP reinforcements:

- Strain in the concrete and the GFRP reinforcement is proportional to the distance from the neutral axis (that is, a plane section before loading remains plane after loading);
- Concrete tensile strength is ignored;
- The maximum usable compressive strain in the concrete is assumed to be 0.003;
- The stress-strain curve of GFRP reinforcement is idealized as linear elastic to failure;
- The stresses in the concrete can be computed from the strains by using stress-strain curves for concrete; and
- There is a perfect bond between the GFRP reinforcement and the concrete.

Balanced Reinforcement Ratio

Existing design guidelines for FRP, such as the ACI-440.1R-06 (ACI 2006) and ISIS Canada (2007), distinguish between concrete crushing and FRP rupture through the balanced reinforcement ratio, ρ_{fb}, where strains in concrete and GFRP bars simultaneously reach their maximum values. This is the common design concept for FRP RC sections. The strain and the stress distribution in the cross-section are shown in Figs. 1(b and c), respectively. In this case, the stress distribution in the concrete can be approximated by Whitney's rectangular stress block [Fig. 1(d)]. By considering equilibrium of internal forces and linear strain distribution assumption, the balanced reinforcement ratio can be expressed as Eq. (1)

$$\rho_{fb} = \frac{0.85\beta_1 f_c'}{f_{fu}} \frac{\varepsilon_{cu} E_f}{f_{fu} + \varepsilon_{cu} E_f} \tag{1}$$

where β_1 = ratio of depth of equivalent rectangular stress block to depth of neutral axis; E_f = elastic modulus for GFRP; f_{fu} = ultimate tensile strength of GFRP; f_c' = cylinder compressive strength of concrete; and ε_{cu} = ultimate compressive strain of concrete, which is assumed to be 0.003 according to ACI 440.1R-06 (ACI 2006). Note that this paper focuses on the short-term behavior of GFRP RC beams, and the degradation of f_{fu} due to exposure to various types of environments was not considered herein.

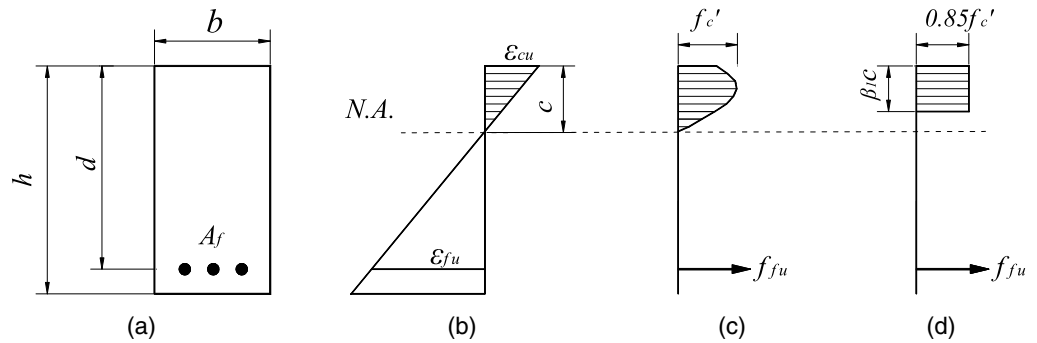

Fig. 1. Balanced failure mode: strain and stress conditions (a) cross section; (b) strain; (c) stress; (d) stress (equivalent)

Table 1. Reinforcement Ratio versus Failure Mode

GFRP reinforcement ratio ρ_f	Failure mode
$\rho_f < \rho_{fb}$	Tension failure
$\rho_{fb} \le \rho_f \le 1.5\rho_{fb}$	Uncertainty
$\rho_f > 1.5\rho_{fb}$	Compression failure

Upper Bound of Reinforcement Ratio for Beams in the Transition Region

The flexural capacity of a GFRP reinforced flexural member is dependent on whether the failure is governed by concrete crushing or GFRP rupture. Theoretically, if the GFRP reinforcement ratio is less than the balanced ratio ($\rho_f < \rho_{fb}$), the GFRP rupture failure mode governs. Otherwise, the concrete crushing failure mode governs ($\rho_f > \rho_{fb}$). Although theoretical delineation of the concrete crushing failure mode of concrete beams is possible, the actual member may not fail as predicted. This mainly is attributed to the uncertainties of material strengths, assumptions made in analysis, and variations in locations of reinforcements and dimensions of concrete sections. For example, if the concrete strength is higher than specified, the member can fail due to FRP rupture. Similarly, if the maximum compressive strain of concrete reaches higher than the assumed value of 0.003 in analysis, the member can fail due to FRP rupture. In this paper, a total of 173 GFRP RC beams tested in flexure were collected from the available experiments. Eq. (1) was performed to predict the flexural failure modes. It was found that 10 beams did not fail in the predicted failure mode, and that there was a transition region where compression failure and tension failure were possible. Therefore, if Eq. (1) is used to distinguish the flexural failure mode, an upper bound of reinforcement ratio for beams in the transition region should be specified. Vijay and GangaRao (2001) proposed a method to determine the upper bound of reinforcement ratio for beams in the transition region, as shown in Eq. (2)

$$\rho^* = \frac{\rho_{fb}}{1 - 3\sigma} \tag{2}$$

where σ is the standard deviation of the ratio between the theoretical flexural capacity and experimental bending capacity of GFRP RC beams failing in compression failure.

The standard deviation σ in Eq. (2) was observed from the comparisons between the theoretical flexural capacity and experimental bending capacity of 90 GFRP RC beams failing in compression with $\rho_f > \rho_{fb}$. It should be noted that all material reduction and safety factors in determining the flexural capacity were set equal to 1.0 in this study. The Appendix lists the specimens that were used to obtain the standard deviation σ. Based on a statistical analysis, the standard deviation σ was taken as 10.9% (see Appendix). Therefore, the upper bound of reinforcement ratio for beams in the transition region ρ^* should be taken as $1.5\rho_{fb}$. The reinforcement ratio of $1.5\rho_{fb}$, which is 50% higher than the balanced failure condition, accounts for the possible tension failure mode due to aforementioned sources of uncertainty. In summary, Table 1 lists the relationship between GFRP reinforcement ratios and failure modes.

Tension Failure Mode

If a beam is designed to fail by GFRP rupture, a minimum amount of reinforcement should be provided to prevent failure upon concrete cracking. According to ACI 440.1R-06 (ACI 2006), the minimum reinforcement ratio is given by Eq. (3)

$$\rho_{f,\min} = \frac{0.41\sqrt{f'_c}}{f_{fu}} \text{ (MPa)} \tag{3}$$

When $\rho_{f,\min} \le \rho_f < \rho_{fb}$, the failure of the member is initiated by rupture of GFRP bar. At failure, the ultimate tensile strain of GFRP, ε_{fu}, is reached and the compressive strain at the extreme compression fiber of concrete, ε_c, does not reach the ultimate compressive strain ε_{cu}. In such a case, the strain and the stress distribution in the cross-section are shown in Figs. 2(b and c), respectively. The stress distribution in the concrete can be approximated with an equivalent rectangular stress block using two strain-dependent and stress-dependent parameters α and β[as shown in Fig. 2(d)]. To compute the equivalent stress block parameters α and β, the stress-strain relationship in concrete needs to be determined. A number of models describing the stress-strain curve of concrete have been proposed. One of commonly used models is the Todeschini model (Todeschini et al. 1964). The equivalent stress block parameters for the Todeschini model are given as (Bank 2006; Nanni et al. 2014)

$$\alpha = \frac{0.90\ln(1 + \varepsilon_c^2/\varepsilon_0^2)}{\beta\varepsilon_c/\varepsilon_0} \tag{4}$$

$$\beta = 2 - \frac{4[\varepsilon_c/\varepsilon_0 - \tan^{-1}(\varepsilon_c/\varepsilon_0)]}{\varepsilon_c/\varepsilon_0 \ln(1 + \varepsilon_c^2/\varepsilon_0^2)} \tag{5}$$

where ε_c = compressive concrete strain and ε_0 = concrete strain at maximum strength as determined from cylinder tests calibrated based on the results reported by Todeschini et al. (1964) as $\varepsilon_0 = 1.71f'_c/E_c$. The concrete modulus E_c is equal to $4{,}700\sqrt{f'_c}$ MPa, according to the ACI 318 building code (ACI 2011).

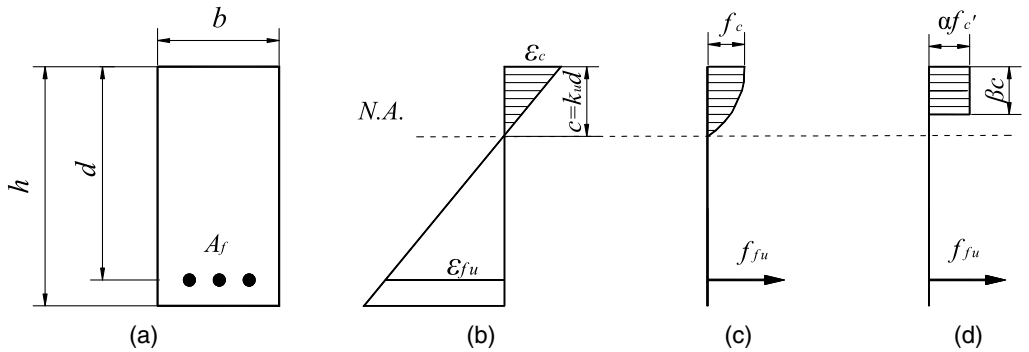

Fig. 2. Tension failure mode: strain and stress conditions (a) cross section; (b) strain; (c) stress; (d) stress (equivalent)

By considering equilibrium of internal forces, Eq. (6) is obtained

$$A_f f_{fu} = \alpha\beta f_c' bc \tag{6}$$

where A_f = area of longitudinal GFRP reinforcement in tension; b = width of beam; and c = distance from extreme compression fiber to the neutral axis.

Referring to the strain distribution shown in Fig. 2(b), one obtains

$$k_u = \frac{c}{d} = \frac{\varepsilon_c}{\varepsilon_c + \varepsilon_{fu}} \tag{7}$$

where d = effective depth and k_u = ratio of the depth of the neutral axis to the effective depth.

Defining the reinforcement index $\omega_f = \rho_f f_{fu}/f_c'$, Eq. (6) can be expressed as

$$k_u = \frac{\omega_f}{\alpha\beta} \tag{8}$$

In order to determine the equivalent parameters α and β, a numerical procedure is required. The procedure is summarized in the following steps:

1. Calculate the minimum reinforcement ratio $\rho_{f,\min}$ from Eq. (3);
2. Assume a value for the concrete strain ε_c at extreme compression fiber of concrete;
3. Calculate the block parameters α and β from Eqs. (4) and (5), respectively;
4. According to the linear strain distribution, determine the value of k_u using Eq. (7);
5. According to the force equilibrium, determine the value of k_u from Eq. (8); and
6. If k_u in step 4 equals the value in step 5, the coefficient k_u is calculated from Eq. (7) or Eq. (8). Otherwise, ε_c should be changed and steps 2 to 5 should be repeated until k_u in step 4 equals the value in step 5.

Repeating the aforementioned procedure for increasing values of the reinforcement ratio ρ_f until the reinforcement ratio ρ_f reaches the balanced reinforcement ratio ρ_{fb}, the corresponding nondimensional equivalent neutral axis depth βk_u can be computed; thus, tables of the reinforcement index ω_f and the nondimensional equivalent neutral axis depth βk_u can be generated.

Based on the described procedure, parametric studies were performed using a wide range of values for design parameters, for example, the elastic modulus of GFRP reinforcements (E_f) ranging from 40 to 60 GPa, ultimate tensile strain of GFRP bars (ε_{fu}) ranging from 0.01 to 0.025, concrete compressive strength (f_c') ranging from 30 to 60 MPa, and GFRP reinforcement ratio (ρ_f) ranging from $\rho_{f,\min}$ to ρ_{fb}.

Fig. 3 presents (as an example) the βk_u coefficient graphically in terms of the reinforcement index ω_f and the ultimate strain of GFRP ε_{fu}, for the particular case of the modulus of elasticity of GFRP $E_f = 40$ GPa and the concrete strength $f_c' = 30$ MPa. The obtained numerical results (as shown in Fig. 3) indicate that the nondimensional equivalent neutral axis depth βk_u is approximately linear with the reinforcement index ω_f. Based on a regression analysis, Eq. (9) for the nondimensional equivalent neutral axis depth βk_u was proposed

$$\beta k_u = \omega_f + \frac{0.14}{1 + 400\varepsilon_{fu}} \tag{9}$$

From the moment equilibrium, the nominal flexural strength of an under-reinforced section can be computed by Eq. (10)

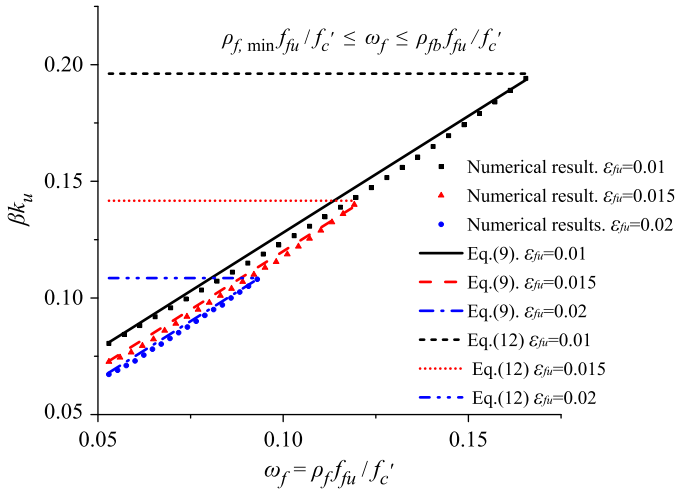

Fig. 3. Variation in nondimensional equivalent neutral axis depth βk_u for tension failure

$$M_n = A_f f_{fu}\left(1 - \frac{\beta k_u}{2}\right) d \tag{10}$$

ACI 440.1R-06 (ACI 2006) also recommended a simplified procedure for failure due to GFRP rupture. This simplification was based on the balanced failure condition, and a constant maximum value for the depth of the compressive stress block was obtained

$$c_b = \frac{\varepsilon_{cu}}{\varepsilon_{cu} + \varepsilon_{fu}} d \tag{11}$$

where c_b = depth of compression zone at balanced strain condition. In this case, the nondimensional equivalent neutral axis depth βk_u can be expressed as

$$\beta k_u = \frac{\beta_1 \varepsilon_{cu}}{\varepsilon_{cu} + \varepsilon_{fu}} \tag{12}$$

Eq. (12) is plotted as the dashed curves in Fig. 3. Note that Eq. (12) obtained from ACI 440.1R-06 (ACI 2006) does not take into account the possible variation in the nondimensional equivalent neutral axis depth βk_u, when there is a change in the reinforcement ratio of the GFRP RC section.

Compression Failure Mode

When $\rho_f \ge 1.5\rho_{fb}$, the failure of the member is initiated by crushing of the concrete and the stress distribution in the concrete can be approximated by Whitney's rectangular stress block. The stresses in GFRP bars at failure, however, are unknown. Based on equilibrium conditions and compatibility conditions (shown in Fig. 4), the following equations can be obtained:

$$M_n = A_f f_f \left(d - \frac{\beta_1 c}{2}\right) \tag{13}$$

$$A_f f_f = 0.85\beta_1 f_c' bc \tag{14}$$

$$f_f = E_f \varepsilon_{cu} \frac{d - c}{c} \tag{15}$$

where f_f = stress in GFRP reinforcement in tension at failure.

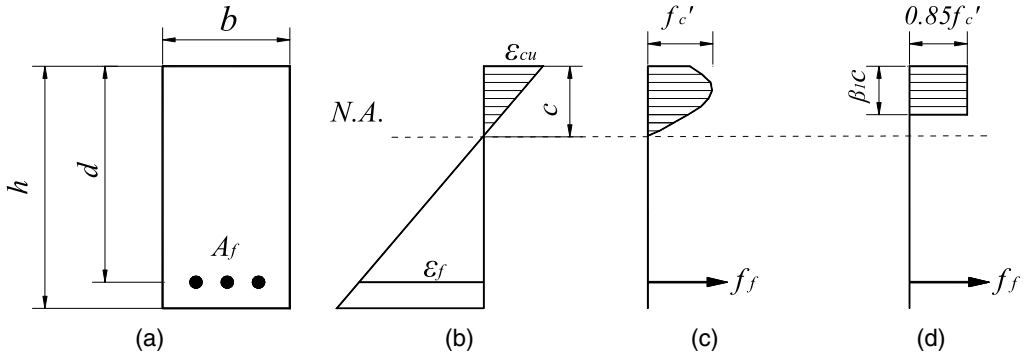

Fig. 4. Compression failure mode: strain and stress conditions (a) cross section; (b) strain; (c) stress; (d) stress (equivalent)

Combining Eqs. (14) and (15) to eliminate c, Eq. (16) is obtained

$$f_f = \left[\sqrt{\frac{(E_f\varepsilon_{cu})^2}{4} + \frac{0.85\beta_1 f_c'}{\rho_f}E_f\varepsilon_{cu}} - 0.5E_f\varepsilon_{cu}\right] \le f_{fu} \quad (16)$$

Substituting f_c' from Eq. (1) into Eq. (16) to eliminate f_c', it can be found that the stress in GFRP at failure f_f is a function of the ultimate tensile stress of GFRP, f_{fu}, and the ratio between the reinforcement ratio and the balanced reinforcement ratio, ρ_f/ρ_{fb}. Based on experimental results of 93 over-reinforced ($\rho_f \ge 1.5\rho_{fb}$) concrete beams, a regression analysis of f_f/f_{fu} was made as a function of ρ_f/ρ_{fb}. This analysis provided the following simplified expression:

$$f_f = f_{fu}(\rho_f/\rho_{fb})^{-0.55} \quad (17)$$

Eq. (17) is plotted as a solid curve in Fig. 5. It is found that the coefficient of determination R^2 of the regression curve is 0.86, which indicates a good correlation between the experimental and the predicted results (Haldar and Mahadevan 2000). Note that a higher GFRP reinforcement ratio leads to less efficient use of the GFRP tensile strength from Fig. 5.

Uncertain Failure Mode

When $\rho_{fb} \le \rho_f < 1.5\rho_{fb}$, the failure mode of GFRP RC beams is uncertain; that is, tension failure and compression failure are possible. Fig. 6 compares the predictions from Eq. (17) against the measured results of 33 beams in the transition region. It can be seen from Fig. 6 that Eq. (17), which is based on the over-reinforced members ($\rho_f > 1.5\rho_{fb}$), generally overestimates the GFRP tensile stress at failure f_f. For the sake of safety and continuity of design equations, a regression curve [Eq. (18)] was chosen close to the lower envelope curve

$$f_f = f_{fu}[1 - 0.23(\rho_f/\rho_{fb} - 1)^{0.2}] \quad (18)$$

Eq. (18) is plotted as a dashed curve in Fig. 6. The coefficient of determination R^2 is 0.82 for Eq. (18), and is 0.70 for Eq. (17). It is clear that Eq. (18) shows a better correlation between the experimental and the predicted results than Eq. (17) does.

Design Recommendations

From the preceding discussions, the stress in GFRP reinforcement at failure can be computed by Eq. (19)

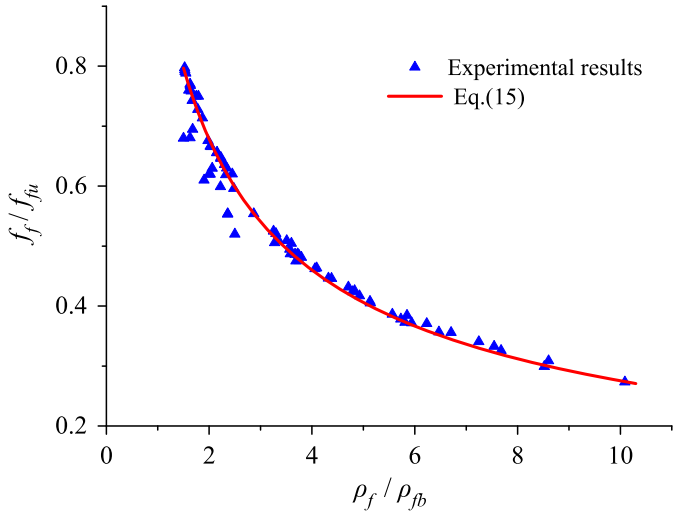

Fig. 5. Relationship between f_f/f_{fu} and ρ_f/ρ_{fb} for compression failure mode

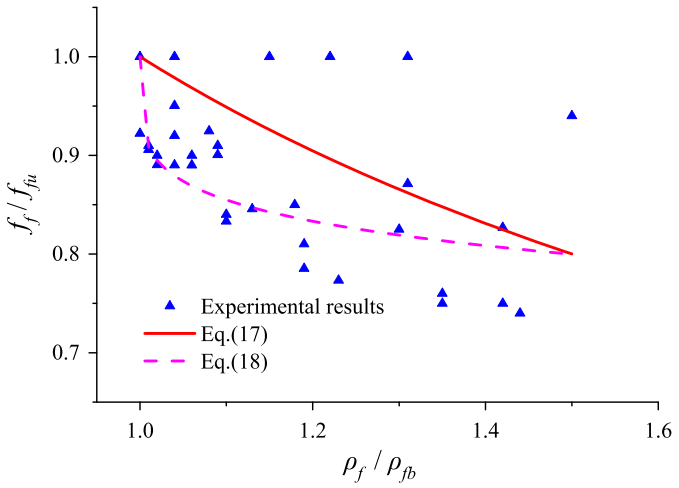

Fig. 6. Relationship between f_f/f_{fu} and ρ_f/ρ_{fb} for uncertain failure mode

$$f_f = \begin{cases} f_{fu} & (\rho_{f\min} \le \rho_f < \rho_{fb}) \\ [1 - 0.23(\rho_f/\rho_{fb} - 1)^{0.2}] f_{fu} & (\rho_{fb} \le \rho_f \le 1.5\rho_{fb}) \\ (\rho_f/\rho_{fb})^{-0.55} f_{fu} & (1.5\rho_{fb} < \rho_f) \end{cases} \quad (19)$$

The design equations previously presented allow the calculation of the nominal moment resistance using Eq. (20)

$$M_n = \rho_f f_f j b d^2 \quad (20)$$

where j = coefficient of the lever arm of the couple force, given by

$$j = \begin{cases} 1 - \dfrac{0.07}{1 + 400\varepsilon_{fu}} - 0.5\dfrac{\rho_f f_f}{f'_c} & (\rho_{f\min} \le \rho_f < \rho_{fb}) \\ 1 - 0.59\dfrac{\rho_f f_f}{f'_c} & (\rho_f \ge \rho_{fb}) \end{cases} \quad (21)$$

Note that Eq. (21) takes into account the variation in the lever arm of the couple force when there is a change in the reinforcement ratio, whether GFRP RC beams fail due to GFRP rupture or concrete crushing.

Verification of Design Equations

A database of 173 GFRP RC beams, including nine beams tested by our research group previously, was used to validate the proposed design equations. The geometrical and material properties of all beams considered are listed in the Appendix. The reinforcement ratio of the beams ranges from 0.21 to 10.09 times the balanced reinforcement ratio ρ_{fb}, which covers a relatively wide range of the reinforcement ratio of GFRP RC beams used in practice. All 173 beams (including 47 under-reinforced beams, 33 beams in the transition region, and 93 over-reinforced beams) were reported to fail in flexure, and satisfied the minimum reinforcement requirements. In addition to the proposed equations, the predictions given by ACI 440 (ACI 2006) equations and FIB Task Group 9.3 (FIB 2007) equations were also compared against the experimental results in the database. It should be noted that all material reduction and safety factors in the design equations considered in this study were set equal to 1.0 for the sake of comparison.

Current Flexural Design Guidelines for GFRP RC Beams

ACI 440.1R-06 (ACI 2006), based on the balanced GFRP reinforcement ratio ρ_{fb}, predicts the nominal flexural capacity M_n of beams reinforced with GFRP bars using Eq. (22) when the reinforcement ratio ρ_f is less than ρ_{fb}, and by applying Eqs. (16) and (23) when the reinforcement ratio ρ_f is greater than ρ_{fb}. Herein, the ultimate compressive strain in concrete ε_{cu} is assumed to 0.003. It should be mentioned that Eq. (22) is derived bassed on the balanced failure condition in which the extreme compression fiber of concrete reaches the ultimate compressive strain, ε_{cu}

$$M_n = \rho_f f_{fu}\left(1 - \frac{\beta_1}{2}\frac{\varepsilon_{cu}}{\varepsilon_{cu} + \varepsilon_{fu}}\right) b d^2 \quad (22)$$

$$M_n = \rho_f f_f \left(1 - 0.59\frac{\rho_f f_f}{f'_c}\right) b d^2 \quad (23)$$

According to FIB Task Group 9.3 (FIB 2007), when the longitudinal GFRP reinforcement ratio ρ_f is below the balanced reinforcement ratio ρ_{fb}, the nominal moment resistance can be achieved by solving Eqs. (24) and (25). If the GFRP reinforcement ratio ρ_f is higher than ρ_{fb}, the nominal moment resistance can be calculated by Eqs. (26) and (27). Herein, the ultimate compressive strain in concrete ε_{cu} is assumed to 0.0035. In this case, calculation of the nominal moment capacity of an under-reinforced section ($\rho_f < \rho_{fb}$) requires use of the nonlinear stress-strain curve of the concrete, and this necessitates an iterative procedure

$$M_n = A_f f_{fd}\left(1 - \frac{\xi}{2}\right) d \quad (24)$$

$$b d \xi \frac{\int_0^{\varepsilon_c} \sigma_c d\varepsilon_c}{\varepsilon_c} = A_f f_{fd} \quad (25)$$

$$M_n = \eta f_{cd} b d^2 (\lambda\xi)\left(1 - \frac{\lambda\xi}{2}\right) \quad (26)$$

$$\xi = \frac{x}{d} = \frac{2\varepsilon_{cu}}{-\varepsilon_{cu} + \sqrt{\varepsilon_{cu}^2 + \frac{4\eta f_{cd}\lambda\varepsilon_{cu}}{\rho_f E_f}} + 2\varepsilon_{cu}} \quad (27)$$

where f_{fd} = design value of tensile strength for GFRP; x = neutral axis depth; f_{cd} = design value of concrete compression strength; λ = factor defining effective height of compression zone; η = factor defining strength deduction factor; ξ = ratio of the neutral axis depth to the effective depth; and σ_c = concrete compressive stress.

Comparison with Design Equations

The Appendix compares the predictions from the proposed equations, ACI 440 (ACI 2006) equations and FIB Task Group 9.3 (FIB 2007) equations against the experimental moment capacities of GFRP RC beams in the database. Table 2 lists the means and standard deviations of the ratio between the predictions and experimental moment strengths of 173 GFRP RC beams ($M_n/M_{\exp}$). Generally, the predictions obtained from the three design approaches are in good agreement with the experimental results.

Table 2. Performance of Flexural Design Equations Considered in This Study

	$M_n/M_{\exp}$		$M_n/M_{\exp}$		$M_n/M_{\exp}$		$M_n/M_{\exp}$	
	$0 < \rho_f < 11\rho_{fb}$ (173 beams)		$\rho_{f,\min} \le \rho_f < \rho_{fb}$ (47 beams)		$\rho_{fb} \le \rho_f \le 1.5\rho_{fb}$ (33 beams)		$\rho_f > 1.5\rho_{fb}$ (93 beams)	
Method	Mean	Standard deviation (%)	Mean	Standard deviation (%)	Mean	Standard deviation (%)	Mean	Standard Deviation (%)
ACI 440 (ACI 2006)	0.94	19	0.91	21	1.05	19	0.94	17
FIB (2007)	1.05	18	0.96	16	1.10	18	1.05	19
Proposed equations	1.01	15	0.96	17	1.01	12	0.99	11

However, the equations proposed in this paper are more predictive than ACI 440 (ACI 2006) and FIB Task Group 9.3 (FIB 2007), in terms of mean value and coefficient of variation of the ratio between the experimental and the predicted values. The mean value obtained (1.01) is the best from all the methods studied. The coefficient of variation obtained (15%) is the lowest of all the methods studied.

Particularly, the influence of failure modes on the accuracy of these design equations was investigated. Table 2 presents the means and the standard deviations of the ratio of computed to experimental moment capacity of under-reinforced beams, beams in the transition region, and over-reinforced beams, respectively. For under-reinforced beams ($\rho_f < \rho_{fb}$), both the proposed equations and FIB Task Group 9.3 (FIB 2007) equations predict the moment capacity of under-reinforced sections with sufficient accuracy. The proposed equations, however, avoid an iterative process. On the other hand, the simplified equation proposed by ACI 440.1R-06 (ACI 2006) gives conservative predictions. For beams in the transition region ($\rho_{fb} \le \rho_f < 1.5\rho_{fb}$), both the ACI 440 (ACI 2006) and FIB Task Group 9.3 (FIB 2007) equations mostly overestimate the load capacity of GFRP RC beams. One of the reasons for these overestimations may be that both of these design guidelines are based on the assumption of concrete crushing. For over-reinforced beams ($\rho_f \ge 1.5\rho_{fb}$), the proposed equations provide the most accurate moment capacity estimations for GFRP RC beams. Meanwhile, ACI 440 equations mostly underestimate the load capacity of over-reinforced beams. This may be attributed to the fact that the maximum concrete crushing strain can reach higher values than what is assumed in analysis.

Conclusions

This paper presents a theoretical investigation on the flexural capacity of concrete beams reinforced with GFRP bars. The following conclusions can be drawn from the studies made:

1. An experimental database including 173 flexural tests on GFRP RC beams available in the literature has been established. Based on a statistical analysis of the experimental database, the upper bound of reinforcement ratio of $1.5\rho_{fb}$ for beams in the transition region is suggested.
2. A simplified yet rational design equation for evaluating flexural capacity of GFRP under-reinforced concrete beam is developed based on rigorous sectional analyses. Moreover, alternative and simple design equations based on regression analyses of the experimental database are developed to predict the flexural capacity of beams in the transition region and over-reinforced beams, respectively.
3. The proposed equations have been applied to predict the results of 173 flexural tests on FRP RC beams. Predictions made by ACI 440 and FIB Task Group 9.3 design equations have been also compared with the experimental results. Analysis of this comparison indicates that ACI 440 design equations give conservative predictions for under-reinforced beams. The proposed design equations are more predictive than ACI 440 and FIB Task Group 9.3 design equations and can be used for design purposes.

It should be mentioned that Eqs. (19)–(21) have been adopted in Shanghai's Construction Standard "Design and Construction of Concrete Structures with Fibre-Reinforced Polymers," which will be published in 2015, in Shanghai, China.

Appendix.

Comparisons between the Theoretical and Experimental Flexural Capacity of GFRP RC Beams

Investigators	Specimen	b (mm)	d (mm)	f'_c (MPa)	f_{fu} (MPa)	E_f (GPa)	ρ_f (%)	ρ_f/ρ_{fb}	$M_{n,\text{exp}}$ (kN m)	$M_{n,\text{pred}}/M_{n,\text{exp}}$ This study	ACI 440	FIB Task Group	Failure mode[a]
Nawy and Neuwerth (1971)	1	89	165	33.1	1,067	50.3	0.20	0.74	5.32	0.93	0.92	0.92	N
	2	89	165	28.2	1,067	50.3	0.20	0.83	4.03	1.23	1.21	0.99	N
	5	89	160	34.6	1,067	50.3	0.26	0.94	5.73	1.05	1.04	1.06	N
	6	89	160	34.6	1,067	50.3	0.26	0.94	5.73	1.05	1.04	1.06	N
	9	89	159	32.6	1,067	50.3	0.31	1.16	6.83	0.87	0.86	0.88	N
	10	89	159	31.2	1,067	50.3	0.31	1.20	3.96	1.40	1.49	1.42	N
	13	89	160	30.9	1,067	50.3	0.36	1.40	4.91	1.36	1.38	1.34	N
	14	89	160	34.2	1,067	50.3	0.36	1.31	6.01	1.13	1.23	1.10	N
	17	89	159	34.2	1,067	50.3	0.42	1.52	8.74	0.86	0.85	0.86	N
	18	89	159	30.9	1,067	50.3	0.42	1.63	6.96	1.03	1.03	1.08	N
Nawy and Neuwerth (1977)	7	127	276	32.4	724	26.2	1.81	5.85	43.71	1.00	1.00	1.06	N
	8	127	276	29.6	724	26.2	1.81	6.23	39.18	1.07	1.07	1.12	N
	9	127	273	29.6	724	26.2	2.19	7.54	47.54	0.93	0.93	0.97	N
	10	127	273	35.1	724	26.2	2.19	6.71	46.34	1.03	1.04	1.05	N
	11	127	274	39.3	724	26.2	2.54	7.25	50.64	1.06	1.06	1.10	N
	12	127	274	30.3	724	26.2	2.54	8.60	46.94	1.02	1.02	1.06	N
Faza (1991)	C4	152	267	28.9	551	45.5	2.49	3.28	54.60	1.21	1.22	1.24	C[c]
	C8	152	268	34.4	551	50.6	1.90	2.03	56.82	1.11	1.20	1.21	C[c]
	C-H5	152	267	44.8	551	45.5	2.49	2.48	74.73	1.07	1.08	1.08	C[c]
	CC	152	267	51.7	551	45.5	2.49	2.32	81.90	1.03	1.03	1.08	C[c]
	EH2	152	273	44.8	737	48.3	0.91	1.47	42.49	1.02	1.00	1.03	C[c]
	EH4	152	269	38.10	896	47.7	0.87	2.23	51.19	0.99	1.00	1.19	T/C
Brown and Bartholomew (1993)	1	152	122	35.9	896	44.8	0.38	1.07	7.09	0.90	0.89	0.95	N
	2	152	122	35.9	896	44.8	0.38	1.07	6.69	0.96	0.94	0.96	N
	4	152	122	35.9	896	44.8	0.38	1.07	7.28	0.87	0.87	0.86	N
	5	152	122	35.9	896	44.8	0.38	1.07	7.40	0.90	0.85	0.89	N
	6	152	122	35.9	896	44.8	0.38	1.07	6.79	0.94	0.93	0.92	N

Appendix (*Continued.*)

Investigators	Specimen	b (mm)	d (mm)	f'_c (MPa)	f_{fu} (MPa)	E_f (GPa)	ρ_f (%)	ρ_f/ρ_{fb}	$M_{n,\text{exp}}$ (kN m)	$M_{n,\text{pred}}/M_{n,\text{exp}}$ This study	ACI 440	FIB Task Group	Failure mode[a]
Benmokrane et al. (1995)	ISO30-2	200	300	42	689	44	1.06	1.75	80.4	0.91	0.9	0.87	C[c]
	KD30-1	200	300	42	689	44	1.06	1.79	50.6	1.24	1.26	1.30	C[c]
	KD30-2	200	300	42	689	44	1.06	1.79	63.8	1.14	1.12	1.24	C[c]
	KD45-1	200	450	52	689	55	0.68	1.04	106.6	1.15	1.24	1.30	C[c]
	KD45-2	200	450	52	689	55	0.68	1.04	113	1.07	1.15	1.09	C[c]
	ISO55-1	200	550	52	689	43	0.55	0.82	177.5	1.06	1.07	1.08	T
	ISO55-2	200	500	43	689	43	0.55	0.92	177.5	1.07	1.07	1.12	T
	KD55-1	200	550	43	689	43	0.55	0.90	146.9	1.11	1.12	1.14	T
	KD55-2	200	550	43	689	43	0.55	0.90	172.5	1.12	1.12	0.87	T
Brown and Bartholomew (1996)	D-1	102	114	35	551	45	1.23	1.43	6.63	1.01	0.99	1.05	C[c]
	D-2	102	102	35	551	45	1.38	1.60	5.91	0.95	0.86	0.96	C[c]
Al-Salloum et al. (1996)	Group 2	200	157	31.3	561	36	3.60	10.0	34.60	0.95	0.53	0.62	C[c]
	Group 3	200	211	31.3	710	43	1.20	3.75	49.07	0.84	0.77	0.88	C[c]
Benmokrane and Masmoudi (1996)	Series 1	200	262	51.7	776	37.7	0.56	1.15	59.25	0.90	0.90	0.89	N
	Series 2	200	262	51.7	776	37.7	0.91	1.87	65.70	0.99	1.02	1.03	N
	Series 3	200	240	45.0	776	37.7	1.51	3.30	73.94	0.87	0.87	0.98	N
	Series 4	200	240	45.0	776	37.7	2.35	5.13	85.61	0.90	0.87	1.00	N
Vijay and GangaRao (1996)	C2	152	270	44.8	568	37.9	1.35	1.65	55.08	1.05	1.09	1.23	C[c]
	C4	152	270	44.8	568	37.9	1.35	1.65	48.64	1.22	1.23	1.32	C[c]
	M1	152	270	31.0	558	37.9	0.96	1.43	50.15	0.89	0.89	0.93	C[c]
	M2	152	270	31.0	558	37.9	1.93	2.87	53.37	1.11	0.92	1.14	C[c]
Benmokrane et al. (1996)	ISO2	200	300	43	690	44	0.23	1.78	80.40	1.17	1.16	1.17	C[c]
	ISO3	200	550	43	690	44	0.17	0.9	177.70	1.26	1.30	1.34	T
	ISO4	200	550	43	690	44	0.14	0.9	177.70	1.26	1.31	1.35	T
Almusallam et al. (1997)	Comp-00	200	191	35.3	885	43.3	1.33	3.80	41.37	0.90	0.83	0.89	C[c]
	Comp-25	200	191	35.3	885	43.3	1.33	3.80	39.06	0.96	0.88	0.89	C[c]
	Comp-50	200	191	36.4	885	43.3	1.33	3.72	39.35	0.96	0.89	0.90	C[c]
	Comp-75	200	191	36.4	885	43.3	1.33	3.72	49.19	0.77	0.76	0.78	C[c]
Sonobe et al. (1997)	GR-1.26-7	200	245	75.8	540	30	1.26	0.61	79.49	0.97	0.91	0.98	T
Zhao et al. (1997)	GB1	152	220	30.0	1,000	45	1.27	4.93	37.62	0.93	0.92	0.96	C[c]
	GB5	152	220	31.2	1,000	45	1.27	4.79	54.22	0.66	0.65	0.70	C[c]
	GB9	152	220	39.8	1,000	45	1.27	4.09	39.98	0.98	0.98	1.08	C[c]
	GB10	152	220	39.8	1,000	45	1.27	4.09	39.76	0.99	0.98	1.08	C[c]
Duranovic et al. (1997)	GB5	150	210	31.2	1,000	45	1.36	5.13	40.30	0.81	0.74	0.93	C[c]
	GB9	150	210	39.8	1,000	45	1.36	4.38	39.73	0.91	0.86	1.10	C[c]
	GB10	150	210	39.8	1,000	45	1.36	4.38	39.50	0.92	0.92	1.11	C[c]
Thériault and Benmokrane (1998)	BC2NB	130	165	53.0	776	38	1.16	2.34	20.00	0.95	0.94	1.07	C[c]
	BC2HA	130	165	57.1	776	38	1.16	2.23	19.70	0.98	0.99	1.12	C[c]
	BC2HB	130	165	57.1	776	38	1.16	2.23	20.60	0.94	0.94	1.10	C[c]
	BC2VA	130	165	97.3	776	38	1.16	1.31	22.70	1.15	1.17	1.18	C[c]
	BC4NB	130	135	46.1	776	38	2.77	5.94	20.60	0.83	0.79	0.89	C[c]
	BC4HA	130	135	53.8	776	38	2.77	5.56	21.00	0.86	0.82	0.92	C[c]
	BC4HB	130	135	53.8	776	38	2.77	5.56	21.40	0.84	0.80	0.85	C[c]
	BC4VA	130	135	93.4	776	38	2.77	3.25	28.40	0.87	0.86	0.95	C[c]
	BC4VB	130	135	93.4	776	38	2.77	3.25	29.50	0.84	0.82	0.92	C[c]
Masmoudi et al. (1998)	CB2B-1	200	265	44.2	618	38	0.56	0.80	57.90	0.80	0.81	0.81	C[b]
	CB2B-2	200	265	44.2	618	38	0.56	0.80	59.80	0.77	0.77	0.78	C[b]
	CB3B-1	200	265	44.2	618	38	0.91	1.31	66.00	0.97	1.00	1.02	C[c]
	CB3B-2	200	265	44.2	618	38	0.91	1.31	64.80	0.98	1.01	1.11	C[c]
	CB4B-1	200	250	38.2	618	38	1.38	2.15	75.40	0.85	0.87	1.01	C[c]
	CB4B-2	200	250	38.2	618	38	1.38	2.15	71.70	0.89	0.89	1.00	C[c]
	CB6B-1	200	250	38.2	618	38	2.15	3.35	84.80	0.90	0.87	1.06	C[c]
	CB6B-2	200	250	38.2	618	38	2.15	3.35	85.40	0.89	0.77	1.06	C[c]
Toutanji and Saafi (2000)	GB1-1	180	268	35	695	40	0.52	1.02	60	0.72	0.72	0.76	C[c]
	GB1-2	180	268	35	695	40	0.52	1.02	59	0.77	0.75	0.84	C[c]
	GB2-1	180	268	35	695	40	0.79	1.55	65	0.80	0.80	0.82	C[c]
	GB2-2	180	268	35	695	40	0.79	1.55	64.3	0.85	0.82	0.87	C[c]
	GB3-1	180	255	35	695	40	1.10	2.15	71	0.76	0.76	0.80	C[c]
	GB3-2	180	255	35	695	40	1.10	2.15	70.5	0.80	0.78	0.81	C[c]
Pecce et al. (2000)	F2	500	185	30	600	42	0.70	1.04	36.8	0.96	1.03	1.07	T[b]
	F3	500	185	30	600	42	1.22	1.53	60.7	0.82	0.78	0.82	T[b]

Appendix (*Continued.*)

Investigators	Specimen	b (mm)	d (mm)	f'_c (MPa)	f_{fu} (MPa)	E_f (GPa)	ρ_f (%)	ρ_f/ρ_{fb}	$M_{n,\text{exp}}$ (kN m)	$M_{n,\text{pred}}/M_{n,\text{exp}}$ This study	ACI 440	FIB Task Group	Failure mode[a]
Al-Sayed et al. (2000)	II	200	210	31.3	700	35.6	3.60	8.52	34.19	1.00	0.93	1.08	C[c]
	III	200	360	31.3	886	43.3	1.20	3.72	45.13	1.00	0.91	1.06	C[c]
	IV	200	300	40.7	700	35.6	1.15	2.30	59.19	1.00	0.97	1.18	C[c]
	V	200	250	40.7	700	35.6	2.87	5.73	57.00	1.00	0.92	1.11	C[c]
Yost et al. (2001)	1FRP1	381	203	27.6	830	41.4	0.12	0.38	11.49	1.01	0.98	1.02	T
	1FRP2	381	203	27.6	830	41.4	0.12	0.38	12.67	0.92	0.89	0.92	T
	1FRP3	381	203	27.6	830	41.4	0.12	0.38	11.49	1.01	0.98	1.02	T
	2FRP1	318	216	27.6	830	41.4	0.13	0.42	13.62	0.91	0.88	0.92	T
	2FRP2	318	216	27.6	830	41.4	0.13	0.42	13.26	0.94	0.91	0.94	T
	2FRP3	318	216	27.6	830	41.4	0.13	0.42	13.06	0.95	0.92	0.96	T
	4FRP1	203	152	27.6	830	41.4	1.27	4.06	15.78	0.92	0.86	0.99	C[c]
	4FRP2	203	152	27.6	830	41.4	1.27	4.06	15.58	0.93	0.88	1.00	C[c]
	4FRP3	203	152	27.6	830	41.4	1.27	4.06	16.29	0.89	0.84	0.95	C[c]
	5FRP1	191	152	27.6	830	41.4	1.35	4.32	16.37	0.86	0.80	0.91	C[c]
	5FRP2	191	152	27.6	830	41.4	1.35	4.32	16.65	0.84	0.79	0.90	C[c]
	5FRP3	191	152	27.6	830	41.4	1.35	4.32	15.78	0.89	0.83	0.95	C[c]
Gao and Benmokrane (2001)	IS2B-1	200	254	39	552	45	0.50	0.42	38.50	0.88	0.69	0.89	T
	IS2B-2	200	254	51	552	45	0.50	0.32	41.00	0.85	0.65	0.84	T
	KD2B-1	200	254	40	513	49	0.50	0.33	52.20	0.67	0.50	0.66	T
	KD2B-2	200	254	40	513	49	0.50	0.33	52.30	0.67	0.50	0.66	T
	IS3B-1	200	254	39	552	45	0.75	0.63	57.20	0.88	1.02	0.88	T
	IS3B-2	200	254	51	552	45	0.75	0.48	59.70	0.85	0.67	0.86	T
	KD3B-1	200	254	40	513	49	0.75	0.50	59.70	0.86	0.66	0.85	T
	KD3B-2	200	254	40	513	49	0.75	0.50	61.60	0.77	0.79	0.77	T
	IS4B-1	200	231	45	552	45	1.10	0.79	61.00	0.95	0.59	0.92	T
	IS4B-2	200	231	45	552	45	1.10	0.79	54.10	1.02	0.97	1.04	T
	KD4B-1	200	231	40	513	49	1.10	0.73	59.70	0.98	1.10	0.93	T
	KD4B-2	200	231	40	513	49	1.10	0.73	67.80	0.83	0.99	0.82	T
	IS6B-1	200	231	45	552	45	1.64	1.19	76.60	0.91	0.87	1.06	T[b]
	IS6B-2	200	231	45	552	45	1.64	1.19	74.70	0.93	0.91	1.09	T[b]
	CB2B-1	200	253	52	618	38	0.71	0.63	57.90	0.96	0.94	0.95	T
	CB2B-2	200	253	52	618	38	0.71	0.63	59.80	0.97	1.02	0.96	T
	CB3B-1	200	253	52	618	38	1.07	0.95	66.00	0.95	0.99	0.97	T
	CB3B-2	200	253	52	618	38	1.07	0.95	64.70	1.00	1.07	1.01	T
	CB4B-1	200	253	52	618	38	1.52	1.35	75.40	1.15	1.09	1.29	T[b]
	CB4B-2	200	253	52	618	38	1.52	1.35	71.70	1.02	1.08	1.25	T[b]
	CB6B-1	200	253	52	618	38	2.27	2.02	84.80	1.10	1.14	1.34	C[c]
	CB6B-2	200	253	52	618	38	2.27	2.02	85.40	1.03	1.13	1.34	C[c]
Wang and Belarbi (2005)	P4G	178	229	48	690	41	2.13	3.51	51	0.88	0.79	1.08	C[c]
	P8G	178	229	48	552	41	3.17	3.60	47	1.10	0.89	1.21	C[c]
	F4G	178	229	30	690	41	2.13	4.71	46	0.83	0.72	0.89	C[c]
	F8G	178	229	30	552	41	3.17	4.83	40	1.09	0.84	1.18	C[c]
Ashour (2006)	Beam2	150	200	27.8	650	38	0.23	0.50	5.89	1.06	0.97	1.07	T
	Beam4	150	250	27.8	650	38	0.17	0.37	7.85	0.99	0.95	1.00	T
	Beam6	150	300	27.8	650	38	0.14	0.30	10.79	0.90	0.85	0.91	T
	Beam8	150	200	50	650	38	0.23	0.34	5.89	1.08	0.99	1.08	T
	Beam10	150	250	50	650	38	0.17	0.25	9.48	0.83	0.8	0.84	T
	Beam12	150	300	50	650	38	0.14	0.21	16.75	0.90	0.78	0.90	T
Saikia et al. (2007)	FG1SOC	180	200	54.2	972	49	0.78	1.53	36.59	1.27	1.24	1.32	N
	FG1GOC	180	200	51.0	972	49	0.78	1.63	35.48	1.27	1.24	1.26	N
	FG1SFPC	180	200	35.9	972	49	0.78	2.06	34.25	1.22	1.16	1.21	N
	FG1GFPC	180	200	31.4	972	49	0.78	2.22	34	1.17	1.11	1.22	N
	FG2SOC	180	200	33.4	464	49.6	1.41	1.00	40.86	1.06	1.11	1.20	N
	FG2SFC	180	200	30.6	464	49.6	1.41	1.06	39.34	1.08	1.11	1.12	N
	FG2GFC	180	200	30.6	464	49.6	1.41	1.06	39	1.09	1.12	1.14	N
Xue et al. (2009)	I-3	150	175	21.65	400	41	0.54	1.00	9.30	1.00	0.77	0.98	T
	I-4	130	175	21.65	400	41	0.62	1.15	7.90	1.17	1.33	1.17	C[c]
	I-5	148	175	21.65	400	41	0.82	1.52	12.80	1.09	1.12	1.06	C[c]
	I-6	134	175	21.65	400	41	0.91	1.69	12.90	1.09	1.05	1.04	C[c]
	II-2	130	175	20.12	400	41	0.62	1.22	7.90	1.17	1.37	1.16	C[c]
	II-3	117	175	20.12	400	41	1.00	1.96	9.30	1.10	1.26	1.06	C[c]
	III-1	120	175	28.59	400	41	1.3	1.81	19.40	0.85	0.85	0.88	C[c]
	IV-1	120	175	47.59	400	41	0.67	0.65	9.30	1.01	0.78	1.02	T
	IV-2	120	175	47.59	400	41	1.35	1.31	21.10	0.92	0.97	0.88	T[b]

Appendix (*Continued.*)

Investigators	Specimen	b (mm)	d (mm)	f'_c (MPa)	f_{fu} (MPa)	E_f (GPa)	ρ_f (%)	ρ_f/ρ_{fb}	$M_{n,\exp}$ (kN m)	$M_{n,\text{pred}}/M_{n,\exp}$ This study	ACI 440	FIB Task Group	Failure mode[a]
Lau and Pam (2010)	G0.8-A90	280	340	36.6	593	40	0.83	1.18	158.80	0.80	0.85	1.00	T[b]
	G2.1-A90	280	340	41.3	582	38	2.07	2.76	237.93	0.87	0.84	1.01	C[c]
	G0.4-A135	280	340	42.3	603	40.2	0.35	0.47	80.40	0.85	0.81	0.83	T
	G0.5-A135	280	340	42.5	603	40.2	0.47	0.63	107.30	0.85	0.81	0.83	T
	G2.1-A135	280	340	33.9	582	38	2.07	3.12	236.78	0.81	0.77	0.90	C[c]
Kassem et al. (2011)	G1-6	200	285	39	617	40	1.6	1.5	77.47	1.12	1.16	0.92	C[c]
	G1-8	200	285	39	617	40	2.2	2.0	86.76	1.13	1.16	0.92	C[c]
	G2-6	200	285	39	747	36	1.4	1.9	71.00	1.14	1.17	0.91	C[c]
	G2-8	200	285	39	747	36	1.9	2.5	84.54	1.17	1.24	0.86	C[c]
El-Nemr et al. (2013)	N2#13G2	200	360	33.5	1,639	67	0.38	2.45	82.78	1.09	1.15	1.31	C[c]
	N3#13G1	200	360	33.5	817	48.7	0.56	1.31	81.34	1.10	1.22	1.37	C[c]
	H2#13G2	200	360	59.1	1,639	67	0.38	1.67	101.59	1.09	1.22	1.47	C[c]
	H3#13G1	200	360	59.1	817	48.7	0.56	0.90	82.58	1.24	1.30	1.38	T
	N5#15G2	200	348	29	1,362	69.3	1.52	7.68	129.32	1.13	1.08	1.24	C[c]
	N6#15G1	200	348	33.5	762	50	1.82	3.67	118.73	1.22	1.19	1.41	C[c]
	H5#15G2	200	348	73.4	1,362	69.3	1.52	3.75	178.54	1.22	1.25	1.32	C[c]
	H6#15G1	200	348	73.4	762	50	1.82	2.02	177.73	1.11	1.14	1.20	C[c]
	N5#15G3	200	348	33.8	1,245	59.5	1.52	6.47	110.58	1.24	1.30	1.32	C[c]
	N2#25G3	200	360	33.8	906	60.3	1.51	3.57	115.93	1.23	1.32	1.26	C[c]
	H5#15G3	200	348	73.4	1,245	59.5	1.52	3.58	188.37	1.09	1.11	1.15	C[c]
	H2#25G3	200	360	73.4	906	60.3	1.51	1.98	189.06	1.13	1.18	1.26	C[c]
—	Mean		—	—	—	—	—	—	—	1.01	0.94	1.05	—
	Standard deviation		—	—	—	—	—	—	—	0.15	0.19	0.18	—
	Standard deviation for concrete beams in compression failure									0.11	—	—	—

[a]Failure modes: C = compression; T = tension; and N = not specified/not clear.
[b]Indicates disagreement between predicted and experimentally observed flexural failure modes.
[c]Results considered for calculation of the standard deviation for ultimate moment capacity of concrete beams.

Acknowledgments

The authors gratefully acknowledge the financial support provided by the National Basic Research Program of China (Project No. 2012CB026201) and the Project of Shanghai Science Technology Commission (No. 14DZ1208302).

Notation

The following symbols are used in this paper:

A_f = area of longitudinal GFRP reinforcement (mm^2);
b = width of beam (mm);
c = distance from extreme compression fiber to the neutral axis (mm);
c_b = depth of compression zone at balanced strain condition;
d = effective depth (mm);
E_c = modulus of elasticity of concrete (MPa);
E_f = modulus of elasticity of GFRP (MPa);
f'_c = cylinder compressive strength of concrete (MPa);
f_{cd} = design value of concrete compression strength (MPa);
f_f = stress in GFRP reinforcement in tension at failure (MPa);
f_{fd} = design value of tensile strength for GFRP (MPa);
f_{fu} = ultimate tensile strength of GFRP (MPa);
j = coefficient of the lever arm of the couple force;
k_u = ratio of the depth of the neutral axis to the effective depth;
$M_{\exp}$ = experimental flexural strength (kN · m);
M_n = nominal flexural strength (kN · m);
x = neutral axis depth (mm);
α and β = compressive stress block parameters;
β_1 = ratio of depth of equivalent rectangular stress block to depth of neutral axis;
σ_c = concrete compressive stress (MPa);
ε_c = compressive concrete strain;
ε_{cu} = ultimate concrete strain;
ε_{fu} = ultimate GFRP strain;
ε_0 = concrete strain at maximum strength;
ρ_f = = GFRP reinforcement ratio;
ρ_{fb} = balanced GFRP reinforcement ratio;
$\rho_{f,\min}$ = minimum GFRP reinforcement ratio;
ω_f = reinforcement index ($\rho_f f_{fu}/f'_c$);
λ = factor defining effective height of compression zone;
η = factor defining strength deduction factor; and
ξ = ratio of the neutral axis depth to the effective depth.

References

ACI (American Concrete Institute). (2006). "Guide for the design and construction of concrete reinforced with FRP bars." *ACI 440.1 R-06*, Farmington Hills, MI.

ACI (American Concrete Institute). (2011). "Building code requirements for structural concrete (ACI 318-11) and commentary." *ACI 318-11*, Farmington Hills, MI.

Almusallam, T. H., Al-Salloum, Y. A., Al-Sayed, S. H., and Amjad, M. A. (1997). "Behavior of concrete beams doubly reinforced by FRP bars."

Proc., 3rd Int. RILEM Symp. on Non-Metallic (FRP) Reinforcement for Concrete Structures, RILEM, Bagneux, France, 471–478.
Al-Salloum, Y. A., Al-Sayed, S. H., Almusallam, H. T., and Amjad, M. A. (1996). "Some design considerations for concrete beams reinforced by glass fiber reinforced plastics (GFRP) bars." *Proc.,1st Int. Conf. on Composites in Infrastructure*, Kluwer Academic, Dordrecht, Netherlands, 318–331.
Al-Sayed, S. H., Al-Salloum, Y. A., and Almusallam, T. H. (2000). "Performance of glass fibre reinforced plastic bars as a reinforcing material for concrete structures." *Compos. Part B*, 31(6–7), 555–567.
Ashour, A. F. (2006). "Flexural and shear capacities of concrete beams reinforced with GFRP bars." *Constr. Build. Mater.*, 20(10), 1005–1015.
Bank, L. C. (2006). *Composites for construction: Structural design with FRP materials*, Wiley, New York.
Barris, C., Torres, L., Turon, A., Baena, M., and Catalan, A. (2009). "An experimental study of the flexural behavior of GFRP RC beams and comparison with prediction models." *Compos. Struct.*, 91(3), 286–295.
Benmokrane, B., Chaallal, O., and Masmoudi, R. (1995). "Glass fiber reinforced plastic (GFRP) rebars for concrete structures." *Constr. Build. Mater.*, 9(6), 353–364.
Benmokrane, B., Chaallal, O., and Masmoudi, R. (1996). "Flexural response of concrete beams reinforced with FRP reinforcing bars." *ACI Struct. J.*, 91(2), 46–55.
Benmokrane, B., and Masmoudi, R. (1996). "FRP C-Bar as reinforcing rod for concrete structures." *Proc., 2nd Int. Conf. on Advanced Composite Materials in Bridges and Structures*, M. El-Badry, ed., Canadian Society of Civil Engineering, Montreal, 177–188.
Brown, V. L., and Bartholomew, C. L. (1993). "FRP reinforcing bars in reinforced concrete members." *ACI Mater. J.*, 90(1), 34–39.
Brown, V. L., and Bartholomew, C. L. (1996). "Long-term deflections of GFRP-reinforced concrete beams." *Fiber Composites in Infrastructure: Proc., 1st Int. Conf. on Composites in Infrastructure ICCI'96*, H. Saadatmanesh and M. R. Ehsani, eds., ICCI, Tucson, AZ, 389–400.
Choi, K., Urgessa, G., Taha, M., and Maji, A. (2008). "Quasi-balanced failure approach for evaluating moment capacity of FRP underreinforced concrete beams." *J. Compos. Constr.*, 10.1061/(ASCE)1090-0268(2008)12:3(236), 236–245.
CSA (Canadian Standards Association). (2002). "Design and construction of building components with fiber-reinforced polymers." *CSA S806-02*, Mississauga, Canada.
Duranavic, N., Pilakoutas, K., and Waldron, P. (1997). "Test on concrete beams reinforced with glass fibre reinforced plastic bars." *Proc., 3rd Int. Symp., Non-Metallic (FRP) Reinforcement for Concrete Structures*, Japan Concrete Institute, Tokyo, 479–486.
El-Nemr, A., Ahmed, E. A., and Benmokrane, B. (2013). "Flexural behavior and serviceability of normal-and high-strength concrete beams reinforced with glass fiber-reinforced polymer bars." *ACI Struct. J.*, 110(6), 1077–1088.
Faza, S. S. (1991). "Bending and bond behavior and design of concrete beams reinforced with fiber reinforced plastic rebars." Ph.D. dissertation, West Virginia Univ., Morgantown, WV, 200.
FIB (Fédération Internationale du Béton). (2007). "FRP reinforcement in RC structures." Lausanne, Switzerland.
Gao, D. Y., and Benmokrane, B. (2001). "Calculation method of flexural capacity of GFRP-reinforced concrete beam." *J. Hydraul. Eng.*, 2001 (9), 73–80 (in Chinese).
Haldar, A., and Mahadevan, S. (2000). *Probability, reliability and statistical method in engineering design*, Wiley, New York.
ISIS Canada (Intelligent Sensing for Innovative Structures, Canadian Network of Excellence). (2007). "Reinforcing concrete structures with fibre reinforced polymers." *Design manual no. 3*, Winnipeg, Canada.
Italian Research Council. (2006). "Guide for the design and construction of concrete structures reinforced with fiber-reinforced polymer bars." *CNR DT-203/2006*, Rome.
Kara, I. F., and Ashour, A. F. (2012). "Flexural performance of FRP reinforced concrete beams." *Compos. Struct.*, 94(5), 1616–1625.
Kassem, C., Farghaly, A. S., and Benmokrane, B. (2011). "Evaluation of flexural behavior and serviceability performance of concrete beams reinforced with FRP bars." *J. Compos. Constr.*, 10.1061/(ASCE)CC.1943-5614.0000216, 682–695.
Lau, D., and Pam, H. J. (2010). "Experimental study of hybrid FRP reinforced concrete beams." *Eng. Struct.*, 32(12), 3857–3865.
MacGregor, J. G. (1997). *Reinforced concrete: Mechanics and design*, Prentice-Hall, Upper Saddle River, NJ.
Masmoudi, R., Thériault, M., and Benmokrane, B. (1998). "Flexural behavior of concrete beams reinforced with deformed fiber reinforced plastic reinforcing rods." *ACI Struct. J.*, 95(6), 665–675.
Nanni, A. (1993). "Flexural behavior and design of RC members using FRP reinforcement." *J. Struct. Eng.*, 10.1061/(ASCE)0733-9445(1993)119:11(3344), 3344–3359.
Nanni, A., Luca, D. A., and Zadeh, H. J. (2014). *Reinforced concrete with FRP bars: Mechanics and design*, CRC Press, New York.
Nawy, E. G., and Neuwerth, G. E. (1971). "Behavior of fiber glass reinforced concrete beams." *J. Struct. Div.*, 97(9), 2203–2215.
Nawy, E. G., and Neuwerth, G. E. (1977). "Fiberglass reinforced concrete slabs and beams." *J. Struct. Div.*, 103(2), 421–440.
Pecce, M., Manfredi, G., and Cosenza, E. (2000). "Experimental response and code models of GFRP RC beams in bending." *J. Compos. Constr.*, 10.1061/(ASCE)1090-0268(2000)4:4(182), 182–190.
Saikia, B., Kumar, P., Thomas, J., Rao, K. S. N., and Ramaswamy, A. (2007). "Strength and serviceability performance of beams reinforced with GFRP bars in flexure." *Constr. Build. Mater.*, 21(8), 1709–1719.
Sonobe, Y., et al. (1997). "Design guidelines of FRP reinforced concrete building structures." *J. Compos. Constr.*, 10.1061/(ASCE)1090-0268(1997)1:3(90), 90–115.
Thériault, M., and Benmokrane, B. (1998). "Effects of FRP reinforcement ratio and concrete strength on flexural behavior of concrete beams." *J. Compos. Constr.*, 10.1061/(ASCE)1090-0268(1998)2:1(7), 7–16.
Todeschini, C. E., Bianchini, A. C., and Kesler, C. E. (1964). "Behavior of concrete columns reinforced with high strength steels." *ACI J.*, 61(6), 701–716.
Toutanji, H. A., and Saafi, M. (2000). "Flexural behavior of concrete beams reinforced with glass fiber-reinforced polymer (GFRP) bars." *ACI Struct. J.*, 97(5), 712–719.
Vijay, P. V., and GangaRao, H. V. S. (1996). "A unified limit state approach using deformability factors in concrete beams reinforced with GFRP bars." *Proc., 4th Materials Conf. on Materials for the New Millennium*, ASCE, Reston, VA, 657–665.
Vijay, P. V., and GangaRao, H. V. S. (2001). "Bending behavior and deformability of glass fibre-reinforced polymer reinforced concrete members." *ACI Struct. J.*, 98(6), 834–842.
Wang, H., and Belarbi, A. (2005). "Flexural behavior of fiber-reinforced concrete beams reinforced with FRP rebars." *Proc., 7th Symp. on FRP in Reinforced Concrete Structures—FRPRCS7, SP-230*, American Concrete Institute, Farmington Hills, MI, 895–914.
Xue, W. C., Wang, X. H., and Zhang, S. L. (2008). "Bond properties of high-strength carbon fiber-reinforced polymer strands." *ACI Mater. J.*, 105(1), 11–19.
Xue, W. C., Zheng, Q. W., and Yang, Y. (2009). "Design recommendations on flexural capacity of FRP reinforced concrete beams." *Eng. Mech.*, 26(1), 79–85 (in Chinese).
Yost, J. R., Goodspeed, C. H., and Schmeckpeper, E. R. (2001). "Flexural performance of concrete beams reinforced with FRP grids." *J. Compos. Constr.*, 10.1061/(ASCE)1090-0268(2001)5:1(18), 18–25.
Yost, J. R., and Gross, S. P. (2002). "Flexure design methodology for concrete beams reinforced with fibre-reinforced polymers." *ACI Struct. J.*, 99(3), 308–316.
Zhao, W., Pilakoutas, K., and Waldron, P. (1997). "FRP reinforced concrete: Cracking behavior and determination." *Proc., 3rd Int. Symp. Non-Metallic (FRP) Reinforcement for Concrete Structures*, Japan Concrete Institute, Tokyo, 439–446.